Automatic Detection of Orientation of Mapped Units via Directional Granulometric Analysis

S. Ashok Vardhan, *Member, IEEE*, B. S. Daya Sagar, *Senior Member, IEEE*, N. Rajesh, *Member, IEEE*, and H. M. Rajashekara, *Member, IEEE*

***Abstract*—Automatic detection of orientation of mapped units via directional granulometries is addressed in this letter. A flat symmetric structuring element (B) of size 3 $\times$ 3 with nine elements, which is a disk in eight-connectivity grid, is decomposed into four 1-D directional structuring elements (B^is). Multiscale opening transformations are performed on each mapped unit with respect to these four directional structuring elements to eventually compute direction-specific morphologic entropy values. Based on these values, the orientations of mapped units are classified into four classes that include those units with orientations of: i) South East-North West (B^1), ii) North-South (B^2), iii) South West-North East (B^3), and iv) East-West (B^4). We demonstrated this approach on five model objects, and nine major river basins extracted from DEM of Indian peninsular. This approach yields quantitative results, based on which the mapped units could be automatically classified into four different orientations.**

***Index Terms*—Directional granulometries, entropy, mathematical morphology, pattern spectrum, remote sensing, shape, water bodies.**

I. Introduction

REMOTELY sensed satellite data and digital elevation models (DEMs) act as main sources to map various units of terrestrial relevance (e.g., surface water bodies, mountain objects, piedmont slopes, and geomorphologic basins). These units possessing varied sizes and shapes are of varied spatial complexities possessing different orientations. There were records that paleochannels could be mapped from high resolution satellite data. We proposed that the orientation of these paleochannels has relationships with orientations of the existing visible water bodies. This observation motivated us to develop an approach to map the distribution of water bodies according to their orientations. Surficial features such as water bodies and their orientations provide clues to map the possible existence of paleochannels. In particular, within flood plain regions, classification of surface water bodies according to their orientation is an important study. It is hypothesized that the classification based on directions of the phenomena (e.g., water bodies) would be a way forward to relate the two distinct phenomena possessing similar directions. Motivation stems from the fact that surface water bodies within a biogeographic boundary possess i) conspicuous shapes of varied geometric composition and ii) different orientations. Morphological constitutions of hydrological and geomorphologic phenomena (e.g., river basins, water bodies, and mountain objects) have direct relationship with their function and process. Hence, categorizing such phenomena that could be mapped from varied data sources, according to their orientations would be a step forward in hydrological and geomorphologic research. With this motivation, automatic detection of orientation of such mapped units via directional granulometries is addressed in this letter.

Mathematical morphology [1], [2] has been applied in the contexts of geosciences, remote sensing, and GISci since last two decades [3]–[15]. Granulometry, a technique of mathematical morphology, is commonly used in image and shape analysis [2], [16]. The ideas stemmed from binary and grayscale granulometries [1], [2], [16], [17] are applied, of late, in the contexts of filtering and segmentation in remotely sensed satellite data [4], [5], [8], [12], [14], [17]. The areal distributions of a specific mapped phenomenon (e.g., water bodies, terrestrial surfaces, geomorphologic basins, etc) under the transformations of multiscale opening and closing—nonlinear filtering techniques popular for filtering foreground and background features in an image X—led to computations of granulometric and antigranulometric indexes, respectively for mapped phenomenon and its background [18]–[20]. The areal changes in foreground (background) features after applying multiscale opening (closing), in other words pattern spectra, provide the shape-size quantities to compute granulometric (antigranulometric) index. These indexes, also termed as entropy like shape-size complexity measures, quantify the surficial roughness [16], [20]. We adopted these ideas to perform directional granulometries further to automatically detect the orientations of the mapped units like river basins.

The organization of this letter is as follows. Section II provides basic morphological transformations. Methodology and its demonstration on a section depicting objects with different orientations and results are given in Section III. Section IV provides experimental results obtained for nine river basins, and concluding remarks in Section V.

II. Basic Morphological Transformations

Set theory based mathematical morphological transformations such as dilation, erosion, opening and closing [1], [2]—that could be performed in discrete Euclidean space (Z^n) by

Manuscript received January 7, 2013; revised February 12, 2013 and March 16, 2013; accepted April 22, 2013. This work was supported by the Indian Statistical Institute under Grant SSIU-01.

S. A. Vardhan is with the Wipro Technologies, Bangalore 560100, India (e-mail: ashokvardhan.sanda@wipro.com).

B. S. D. Sagar and N. Rajesh are with the Systems Science and Informatics Unit (SSIU), Indian Statistical Institute-Bangalore Centre, Bangalore 560059, India (e-mail: bsdsagar@isibang.ac.in).

H. M. Rajashekara is with the Central Computer Centre (CCC), Indian Statistical Institute-Bangalore Centre, Bangalore 560059, India (e-mail: raja@isibang.ac.in).

Color versions of one or more of the figures in this paper are available online at http://ieeexplore.ieee.org.

Digital Object Identifier 10.1109/LGRS.2013.2260127

using translations, unions, and intersections—are important in processing and analysis of binary, grayscale, and color images. These transformations, which are of nonlinear nature, have been intensely employed in the areas of remotely sensed satellite data processing, thematic map retrieval, map analysis, information reasoning and visualization, and in developing map-based models. As the present study involves binary morphological transformations, we restrict this section to explain only essential binary morphological transformations that include dilation (1), erosion (2), opening (3), and their multiscale versions (4)–(6). Let X be a raster image depicting a theme and no-theme in a noise-free format. Such a theme consists of various disjointed connected components (X^k), and $\bigcup_{k=1}^{K} X^k = X$. Let B be a structuring element with certain characteristic information employed to probe X and X^c to retrieve morphological descriptors.

A. Dilation

The Boolean OR transformation of X by B is equivalent to the Minkowski set addition $\oplus$, of X by B. This operation that expands image object is also called dilation of X by B

$$X \oplus B = \{x : B_x \cap X \neq \emptyset\} = \bigcup_{b \in B} \mathrm{X}_b \tag{1}$$

where $\oplus$ is a symbol for morphologic dilation, $\mathrm{X}_b = \{x + \hat{b} : x \in X\}$ is the *translation* of X along the vector $\boldsymbol{b}$, and $B = \{x : -x \in B\}$ is the symmetric of B with respect to the origin.

B. Erosion

The Boolean AND transformation of X by $B = \hat{B}$ is equivalent to the Minkowski set subtraction $\ominus$, of X by B. This operation that shrinks the input image object is called *erosion* of X by B

$$X \ominus B = \{x : B_x \subseteq X\} = \bigcap_{b \in B} X_{-b}. \tag{2}$$

C. Opening

Morphological opening transformation, which is an idempotent transformation, involves morphological erosion followed by dilation of X by B as explained in

$$(X \circ B) = (X \ominus B) \oplus B \tag{3}$$

where $\circ$ denotes symbol for morphologic opening. We shall hereafter denote the erosion, the dilation and the opening of X by B, respectively by $(X \ominus B)$, $(X \oplus B)$ and $(X \circ B)$.

D. Multiscale Morphological Transformations

Multiscale morphological transformations (4)–(6) can be performed by varying the size of *structuring element* nB, where $n = 0, 1, 2, \ldots, N$. Dilation, erosion, and opening can also be performed iteratively, as follows:

$$(X \oplus nB) = [(X \oplus B) \oplus B \oplus \cdots \oplus B] \tag{4}$$
$$(X \ominus nB) = [(X \ominus B) \ominus B \ominus \cdots \ominus B] \tag{5}$$
$$(X \circ nB) = [(X \ominus B) \ominus B \ominus \cdots \ominus B] \oplus B \oplus B \oplus \cdots \oplus B. \tag{6}$$

The reader is requested to refer to [2], [16] for a more detailed exposition of this fundamental transformation together with its algebraic properties.

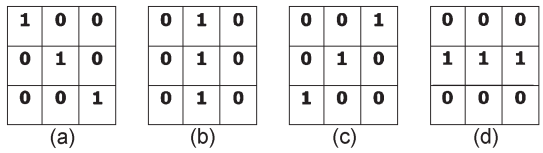

Fig. 1. Directional structuring elements. (a) B^1. (b) B^2. (c) B^3. (d) B^4.

E. Directional Structuring Elements

Structuring element (B) of primitive size 3×3 with nine elements, square in shape, and symmetric about the origin could be decomposed into four directional structuring elements (Fig. 1). These directional structuring elements—respectively denoted as B^1, B^2, B^3, and B^4, are with NW-SE, N-S, NE-SW and E-W directions, and are symmetric about the origin—satisfy following properties:

i) $(B^1 \cup B^2 \cup B^3 \cup B^4) = B$,
ii) $(X \oplus (B^1 \cup B^2 \cup B^3 \cup B^4)) = (X \oplus B)$,
iii) $(X \ominus (B^1 \cup B^2 \cup B^3 \cup B^4)) = (X \ominus B)$,
iv) $(X \circ (B^1 \cup B^2 \cup B^3 \cup B^4)) = (X \circ B)$,
v) $B^i \oplus B^i \oplus \cdots \oplus B^i = nB^i, \bigcup_{i=1}^{4}(nB^i) = nB$,
vi) $(X \ominus (\bigcup_{i=1}^{4}(nB^i))) = (X \ominus nB)$,
vii) $(X \oplus (\bigcup_{i=1}^{4}(nB^i))) = (X \oplus nB)$,
viii) $(X \circ (\bigcup_{i=1}^{4}(nB^i))) = (X \circ nB)$.

III. Methodology and Model Demonstration

Recursive application of morphological opening (closing) of a set X by sequentially changing the size of structuring element B, without changing other characteristic information such as the shape, orientation, and symmetry leads to granulometric (anti-granulometric) analysis. Such granulometric (anti-granulometric) analysis provides: i) shape-size content, ii) shapiness index, and iii) morphological entropy, in other words, roughness of foreground (background) of set X with respect to B.

A. Granulometry

The main objective of this study is filtering the objects according to their orientations. Granulometric principle is the main idea involved in automatically detecting the objects general orientation. An equation to compute granulometric index (H(X/B)), in other words morphological entropy, of a set (object) involves: i) multiscale morphological opening (6); ii) cardinality of sets morphologically opened at multiple scales; iii) logical difference between the successive opened sets; and iv) probability distribution values. Equation (7) to compute granulometric index is given

$$H(X/B) = -\sum_{n=0}^{N} p_n \log p_n \tag{7}$$

where

$$p_n = \frac{A((X \circ nB) \backslash (X \circ (n+1)B))}{A(X)}, \qquad n = 0, 1, 2, \ldots, N \tag{8}$$

where $A(.)$ is the cardinality of the set, in other words, the area of set in pixel units.

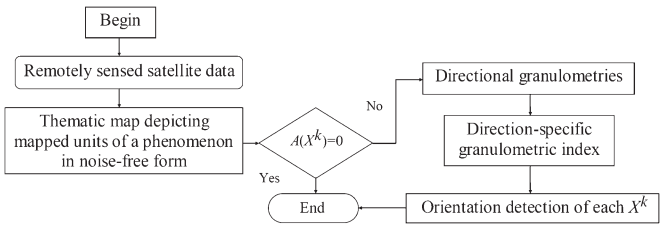

Fig. 2. Flowchart of the proposed procedure.

B. Directional Granulometry

Instead of choosing a structuring element that is a circle in eight connectivity grid, four directional structuring elements (B^i), where $i = 1, 2, 3, 4$ that are symmetric about the origins are considered to compute p_n and $H(X/B^i)$. In turn, (7) and (8) would take the form of (9) and (10)

$$H(X^k/B^i) = -\sum_{n=0}^{N} p_n \log p_n \tag{9}$$

where

$$p_n = \frac{A\left((X^k \circ nB^i) \setminus \left(X^k \circ (n+1)B^i\right)\right)}{A(X^k)} \tag{10}$$

where k, n and i, respectively denote index of connected component, size of structuring element, and index of directional structuring element. $H(X^k/B^i)$ computed according to (9) for all i would yield orientation of X^k, X^k_{ori}, as per

$$X^k_{ori} = \left\{ i : \max_{\forall i} \left(H(X^k/B^i)\right) \right\}. \tag{11}$$

Morphological entropy of X^k is B^i dependent. The B^i with which the X^k yields larger value of morphological entropy has an orientation similar to that X^k that is subjected to granulometries with respect to four B^is with four different orientations and the four orientation-specific morphologic entropies are constructed.

C. Model Demonstration

Sequential steps in flowchart (Fig. 2) enable on how the thematic units mapped from remotely sensed data can be subjected to directional granulometries categorize the thematic units according to their orientations.

To automatically detect orientation of mapped objects according to directional granulometric analysis (Fig. 2), we consider a synthetic section consisting of five objects, denoted with X^1, X^2, X^3, X^4, and X^5 being a circular object (Fig. 3).

Multiscale morphological openings are performed on each X^k with respect to four directional structuring elements. Selected snapshots of X^2 subject to multiscale openings by B^1, B^2, B^3, and B^4 are shown in Fig. 4.

For better understanding, the evolution of four objects under the influence of multiscale opening, with respect to the structuring elements that have orientations similar to the four objects, are shown (Fig. 5). Pattern spectrum of the each X^k with respect to the directional structuring element (B^i) was determined according to (10). The pattern behaviors of the X^ks oriented in different directions could be seen. The changes in areal distribution of these five spatial objects under the influence of recursive multiscale opening with respect to four directional structuring elements are shown in Fig. 6. The slow evolutionary patterns with respective directional structuring elements are obvious as convex graphical patterns (Fig. 6).

Morphological entropy of an object enables spatial complexity of such an object. These morphological entropy values depend upon the characteristic information of structuring element. There would be n-number of morphological entropy values for an object that is subjected to granulometries with respect to

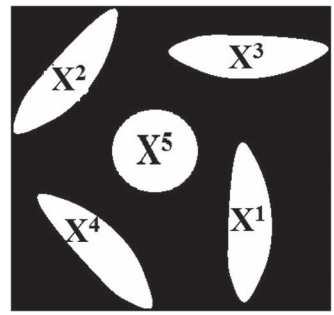

Fig. 3. X^1, X^2, X^3, X^4, and X^5 of a set X—oriented in different directions.

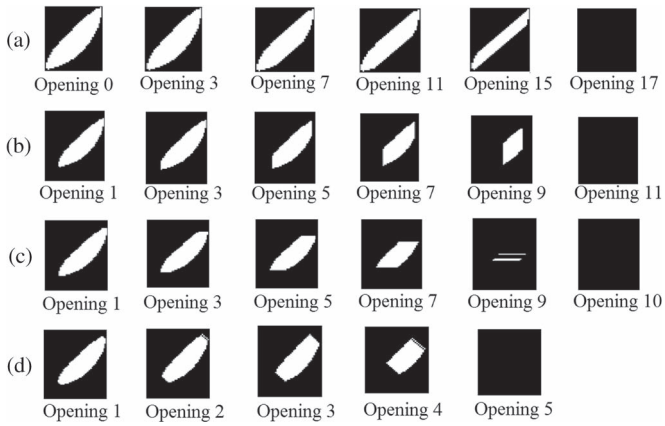

Fig. 4. Evolution of X^2 under recursive opening cycles with respect to (a) B^3, (b) B^2, (c) B^4, and (d) B^1. B^3 took more number of opening cycles to vanish X^2, further attributing that the orientations of X^2 and B^3 are similar.

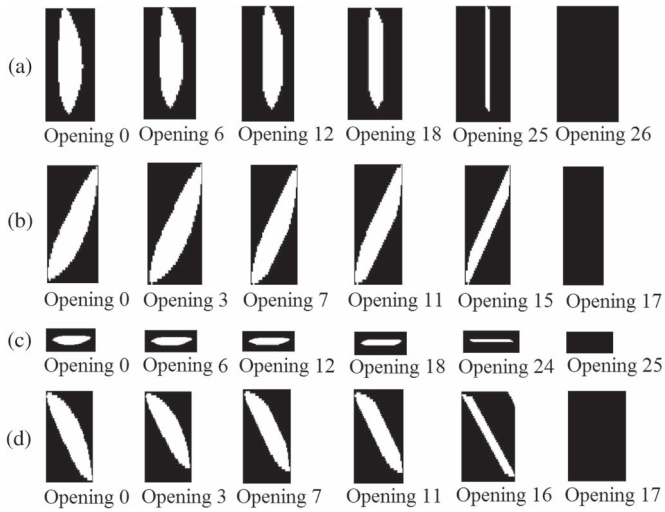

Fig. 5. Evolution of X^k of Fig. 3 under opening cycles by means of structuring elements (B^{i}) of similar orientation. Pattern behaviors under multiscale opening of (a) X^1 by B^2, (b) X^2 by B^3, (c) X^3 by B^4, and (d) X^4 by B^1.

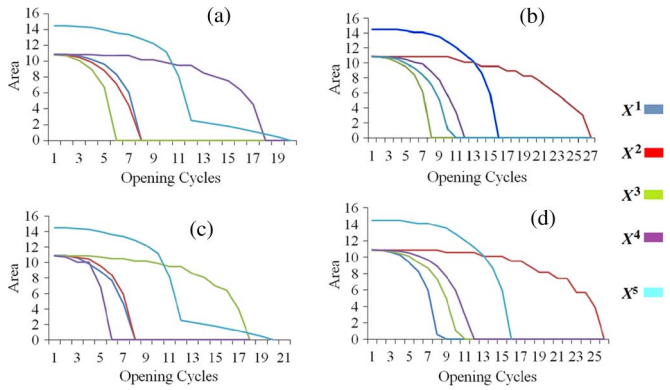

Fig. 6. Size distribution pattern under multiscale morphological opening of $X^k = X^1, X^2, X^3, X^4$, and X^5 by means of (a) B^1, (b) B^2, (c) B^3, and (d) B^4.

TABLE I
GRANULOMETRIC INDEXES OF THE FIVE OBJECTS

Object	(B^1)	(B^2)	(B^3)	(B^4)
X^1	0.79(06)	**1.89(25)**	0.68(06)	0.89(07)
X^2	0.39(04)	0.63(10)	**0.82(16)**	0.55 (09)
X^3	0.76(06)	0.73(06)	0.82(06)	**1.8(24)**
X^4	**0.83(16)**	0.63(09)	0.56(04)	0.39(10)
X^5	0.9(19)	0.7(15)	0.9(19)	0.7(15)

n number of dissimilar structuring elements. For every X^k, morphological entropy was calculated according to (9) with respect to each directional structuring element.

Table I depicts granulometric indexes. The higher the index yields, the higher is the smoothness obtained with respect to that specific B^i. The B^i that yields higher granulometric index for X^k, the corresponding "i" direction is the direction of X^k. The values in the parentheses (Table I) denote the number of opening cycles taken to vanish X^k. This number is dependent upon characteristics of B^i and X^k. It is obvious that the higher morphological entropy the higher the similarity in orientation between X^k and B^i. For the spatial objects, four different entropy values are obtained (Table I) as we considered four different directional structuring elements. Exceptional cases include highly symmetric objects (e.g., ellipse shown as X^5). More number of directions could be identified (considered) by considering increasing sizes of primitive structuring elements (B) that pave ways to see more directional options.

IV. EXPERIMENTAL RESULTS AND DISCUSSION

Application of directional granulometries–explained in the previous section–is extended to automatically detect the orientations of nine river basins (Fig. 7) mapped from coarse resolution DEMs derived from remotely sensed satellite data.

A. Orientation of Nine River Basins

The nine basins situated in the lower half of the Indian peninsular include *Cauvery, Godavari, Krishna, Pennar, Palar, Periyar, Tambarpani, Tapati*, and *Vamsadhara*. These basins have i) irregular shapes, ii) varied sizes, and iii) different orientations.

When the recursive multiscale openings are performed with respect to four B^is on each basin, it is observed that the basin

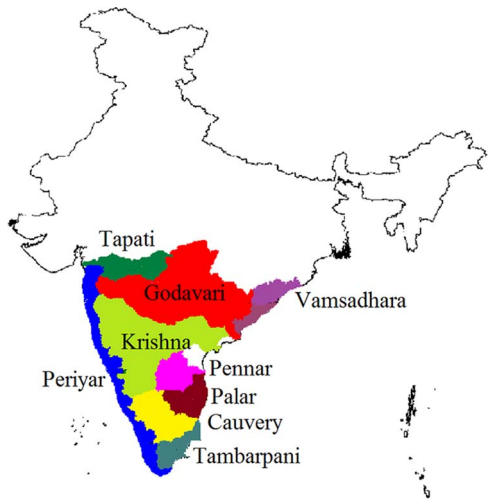

Fig. 7. Nine river basins partitioned from DEM of coarse resolution.

TABLE II
ENTROPY VALUES OF BASINS WITH DIFFERENT ORIENTATIONS

Basins	(B^1)	(B^2)	(B^3)	(B^4)
Cauvery	1.62(141)	1.87 (178)	1.6 (94)	1.86 (172)
Godavari	1.8(127)	1.82 (145)	1.79 (123)	1.92 (240)
Krishna	1.75(111)	1.94 (167)	1.86 (133)	1.91 (211)
Palar	1.83(119)	1.86 (172)	1.85 (132)	1.87 (167)
Pennar	1.76(116)	1.77 (175)	1.73 (133)	1.80 (209)
Periyar	1.31(28)	1.59 (71)	1.1 (17)	1.1 (17)
Tambarpani	1.61(67)	1.68 (109)	1.87(155)	1.74 (119)
Tapati	1.71(96)	1.79 (115)	1.60 (98)	1.87 (319)
Vamsadhara	1.54(54)	1.76 (101)	1.86 (165)	1.81 (110)

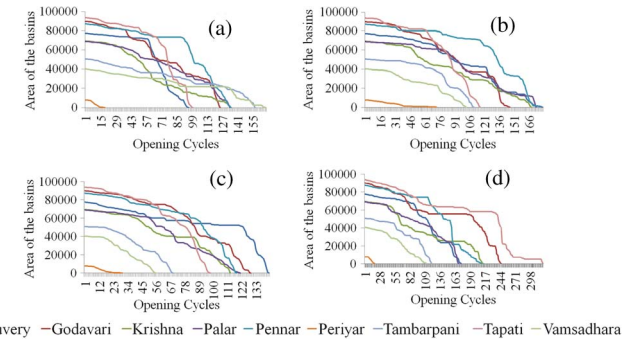

Fig. 8. Size (areal) distribution pattern under multiscale morphological opening of nine river basins with respect to (a) B^1, (b) B^2, (c) B^3, and (d) B^4. On y-axis, the values denote areas in pixel units.

with orientation similar to B^i took more number of iterations [values in parentheses (Table II)] to vanish completely. The opening cycle count is more for such a basin, when compared with the other basins. The minimum number of opening cycles required, to completely vanish the basins, with respect to each directional structuring element is mentioned in parentheses (Table II). The pattern spectra for each basin with respect to four B^is are shown in Fig. 8.

For every opening iteration, area, entropy, pattern spectrum and granulometric indexes are computed according to (9), (10). From Fig. 8, it is evident that, basins which took more iterations during the recursive openings, are oriented in the direction similar to the corresponding structuring element involved in opening process. For instance, when structuring element B^2 is employed on all the nine basins, Cauvery basin took more

TABLE III
COMPARATIVE RESULTS

BASINS	ORIENTATIONS		
	LINEAR DIRECTION METHODS		DIRECTIONAL GRANULOMETRY
	FROM - TO	WITHOUT FROM-TO	
Cauvery	N-S	E-W	N-S
Godavari	N-S	E-W	E-W
Krishna	N-S	E-W	N-S
Palar	N-S	E-W	E-W
Pennar	N-S	E-W	E-W
Periyar	N-S	NW-SE	N-S
Tambarpani	N-S	NE-SW	NE-SW
Tapati	N-S	E-W	E-W
Vamsadhara	N-S	NE-SW	NE-SW

iterations to erode. The entropy values computed with respect to four B^is for each basin are given in Table II. From Table II, it is observed that, *Cauvery, Krishna, Periyar* are oriented in North-South direction, which is similar to the direction of B^2. *Tambarpani* and *Vamsadhara* are oriented in direction similar the B^3. *Godavari*, *Palar*, *Pennar*, and *Tapati* are oriented in direction similar to the B^4.

B. Comparisons

Linear Directional Mean tool, available in ArcGIS identifies the general direction for input feature class that must be a line or a polyline. When measuring direction, this tool, which considers the first and last points in a line, does not consider all of the vertices along a line. When this tool is applied on the nine basins (Fig. 7), the observed directions of these basins are in contrast to the original orientations computed using proposed directional granulometric analysis. The directions obtained for boundaries, which are in polyline forms, of basins are shown in Table III. Orientations obtained by three different approaches have been compared (Table III).

Most of the mapped units that are in raster format act as better inputs for developing spatiotemporal models to explain the dynamical behaviors of phenomena and processes. Creating a bounding box (or) convex hull of X^k that approximates the X^k, and computing long-axis involve significant computation. But such approximations lead to erroneous results when X^k is in contorted form. It is convincing that the proposed directional granulometries in automatically detecting orientation is more stable than the other tools available elsewhere.

V. CONCLUSION

Study of behavior of patterns (objects) mapped from spatial data (e.g., remotely sensed satellite image) via directional granulometries provides a solution to automatically detect the orientations of mapped objects. This approach yields quantitative indexes to categorize the spatial objects (X^k) according to orientation, and is better than those methods which involve approximations. As the X^k considered are in raster form, this proposed method, which can be generalized and can be extended to spatial fields (e.g., grayscale images), is stable due to the fact that i) every pixel of each spatial object would involve in the process of multiscale opening, and ii) shape-size content of the object is investigated with respect to B^i.

ACKNOWLEDGMENT

Authors gratefully acknowledge useful suggestions made by Editor-In-Chief Prof. P. Gamba, Associate Editor, two anonymous reviewers and that significantly strengthened the manuscript.

REFERENCES

[1] G. Matheron, *Random Sets and Integral Geometry*. Hoboken, NJ, USA: Wiley, 1975.
[2] J. Serra, *Image Analysis and Mathematical Morphology*. London, U.K.: Academic, 1982.
[3] B. S. D. Sagar, G. Gandhi, and B. S. P. Rao, "Applications of mathematical morphology on water body studies," *Int. J. Remote Sens.*, vol. 16, no. 8, pp. 1495–1502, Mar. 1995.
[4] M. Pesaresi and J. A. Benediktsson, "A new approach for the morphological segmentation of high-resolution satellite imagery," *IEEE Trans. Geosci. Remote Sens.*, vol. 39, no. 2, pp. 309–320, Feb. 2001.
[5] J. A. Benediktsson, M. Pesaresi, and K. Arnason, "Classification and feature extraction for remote sensing images from urban areas based on morphological transformations," *IEEE Trans. Geosci. Remote Sens.*, vol. 41, no. 9, pp. 1940–1949, Sep. 2003.
[6] B. S. D. Sagar and L. Chockalingam, "Fractal dimension of non-network space of a catchment basin," *Geophys. Res. Lett.*, vol. 31, no. 12, p. L12 502, Jun. 2004.
[7] L. T. Tay, B. S. D. Sagar, and H. T. Chuah, "Analysis of geophysical networks derived from multiscale digital elevation models: A morphological approach," *IEEE Geosci. Remote Sens. Lett.*, vol. 2, no. 4, pp. 399–403, Oct. 2005.
[8] M. D. Mura, J. A. Benediktsson, F. Bovolo, and L. Bruzzone, "An unsupervised technique based on morphological filters for change detection in very high resolution images," *IEEE Geosci. Remote Sens. Lett.*, vol. 5, no. 3, pp. 433–437, Jul. 2008.
[9] X. Huang, L. P. Zhang, and L. Wang, "Evaluation of morphological texture features for mangrove forest mapping and species discrimination using multispectral IKONOS imagery," *IEEE Geosci. Remote Sens. Lett.*, vol. 6, no. 3, pp. 393–397, Jul. 2009.
[10] B. S. D. Sagar, "Visualization of spatiotemporal behavior of discrete maps via generation of recursive median elements," *IEEE Trans. Pattern Anal. Mach. Intell.*, vol. 32, no. 2, pp. 378–384, Feb. 2010.
[11] S. Aksoy and R. G. Cinbis, "Image mining using directional spatial constraints," *IEEE Geosci. Remote Sens. Lett.*, vol. 7, no. 1, pp. 33–37, Jan. 2010.
[12] M. D. Mura, A. Villa, J. A. Benediktsson, J. Chanussot, and L. Bruzzone, "Classification of hyperspectral images by using extended morphological attribute profiles and independent component analysis," *IEEE Geosci. Remote Sens. Lett.*, vol. 8, no. 3, pp. 542–546, May 2011.
[13] H. M. Rajashekara, P. Vardhan, and B. S. D. Sagar, "Generation of zonal map from point data via weighted skeletonization by influence zone," *IEEE Geosci. Remote Sens. Lett.*, vol. 9, no. 3, pp. 403–407, May 2012.
[14] M. Pedergnana, P. R. Marpu, M. D. Mura, J. A. Benediktsson, and L. Bruzzone, "Classification of remote sensing optical and LiDAR data using extended attribute profiles," *IEEE J. Sel. Topics Signal Process.*, vol. 6, no. 7, pp. 856–865, Nov. 2012.
[15] B. S. D. Sagar, N. Rajesh, S. A. Vardhan, and P. Vardhan, "Metric based on morphological dilation for the detection of spatially significant zones," *IEEE Geosci. Remote Sens. Lett.*, vol. 10, no. 3, pp. 500–504, May 2013.
[16] P. Maragos, "Pattern spectrum and multiscale shape representation," *IEEE Trans. Pattern Anal. Mach. Intell.*, vol. 11, no. 7, pp. 701–716, Jul. 1989.
[17] V. Morard, P. Dokládal, and E. Decencière, "One-dimensional openings, granulometries and component trees in $\mathcal{O}(1)$ per pixel," *IEEE J. Sel. Topics Signal Process.*, vol. 6, no. 7, pp. 840–848, Nov. 2012.
[18] B. S. D. Sagar, M. Venu, and B. S. P. Rao, "Distributions of surface water bodies," *Int. J. Remote Sens.*, vol. 16, no. 16, pp. 3059–3067, Nov. 1995.
[19] T. Barata and P. Pina, "A morphological approach for feature space partitioning," *IEEE Geosci. Remote Sens. Lett.*, vol. 3, no. 1, pp. 173–177, Jan. 2006.
[20] L. T. Tay, B. S. D. Sagar, and H. T. Chuah, "Granulometric analysis of basin-wise DEMs: A comparative study," *Int. J. Remote Sens.*, vol. 28, no. 15, pp. 3363–3378, Aug. 2007.